

A passively mode-locked fiber laser at 1.54 μm with a fundamental repetition frequency reaching 2 GHz

J. J. McFerran, L. Nenadović, W. C. Swann, J. B. Schlager and N. R. Newbury

Optoelectronics Division, National Institute of Standards and Technology, 325 Broadway, MS 815.03, Boulder, Colorado 80305, USA.

mcferran@boulder.nist.gov

Abstract: We demonstrate a fundamentally mode-locked fiber laser with a repetition frequency in excess of 2 GHz at a central wavelength of 1.535 μm . Co-doped ytterbium-erbium fiber provides the gain medium for the laser, affording high gain per unit length, while a semiconductor saturable absorber mirror (SAM) provides the pulse shaping mechanism in a standing wave cavity. Results are shown confirming cw mode-locking for 1 GHz and 2 GHz repetition frequency systems. The response of the frequency comb output to pump power variations is shown to follow a single pole response. The timing jitter of a 540 MHz repetition-rate laser has been suppressed to below 100 fs through phase-lead compensated feedback to the pump power. Alternatively, a single comb line of a 850 MHz repetition-rate laser has been phase-locked to a narrow linewidth cw laser with an in-loop phase jitter of 0.06 rad². The laser design is compatible with low-noise oscillator applications.

OCIS codes: (140.3510) Lasers, fiber; (140.4050) Mode-locked lasers; (120.3930) Metrological instrumentation; (230.0250) Optoelectronics.

References and links

1. I. Coddington, W. C. Swann, L. Lorini, J. C. Bergquist, Y. L. Coq, Q. Q. C. W. Oates, K. S. Feder, J. W. Nicholson, P. S. Westbrook, S. A. Diddams, and N. R. Newbury, "Coherent optical link over hundreds of metres and hundreds of terahertz with subfemtosecond timing jitter," *Nature Photonics* **1**, 283 (2007).
2. W. C. Swann, J. J. McFerran, I. Coddington, N. R. Newbury, I. Hartl, M. E. Fermann, P. S. Westbrook, J. W. Nicholson, K. S. Feder, C. Langrock, and M. M. Fejer, "Fiber-laser frequency combs with sub-hertz relative linewidths," *Opt. Lett.* **31**, 3046 (2006).
3. T. R. Schibli, K. Minoshima, F.-L. Hong, H. Inaba, A. Onae, H. Matsumoto, I. Hartl, and M. E. Fermann, "Frequency metrology with a turnkey all-fiber system," *Opt. Lett.* **29**, 2467 (2004).
4. P. Kubina, P. Adel, F. Adler, G. Grosche, T. W. Hänsch, R. Holzwarth, A. Leitenstorfer, B. Lipphardt, and H. Schnatz, "Long term comparison of two fiber based frequency comb systems," *Opt. Express* **13**, 904 (2005).
5. F. Adler, K. Moutzouris, A. Leitenstorfer, H. Schnatz, B. Lipphardt, G. Grosche, and F. Tauser, "Phase-locked two-branch erbium-doped fiber laser system for long-term precision measurements of optical frequencies," *Opt. Express* **12**, 5872 (2004).
6. A. Schliesser, M. Brehm, F. Keilmann, and D. van der Weide, "Frequency-comb infrared spectrometer for rapid, remote chemical sensing," *Opt. Express* **13**, 9029 (2005).
7. F. Keilmann, C. Gohle, and R. Holzwarth, "Time-domain mid-infrared frequency-comb spectrometer," *Opt. Lett.* **29**, 1542 (2004).
8. S. Schiller, "Spectrometry with frequency combs," *Opt. Lett.* **27**, 766 (2002).
9. W. C. Swann and N. R. Newbury, "Frequency-resolved coherent lidar using a femtosecond fiber laser," *Opt. Lett.* **31**, 826 (2006).
10. J. McKinney, D. Leaird, and A. Weiner, "Millimeter-wave arbitrary waveform generation with a direct space-to-time pulse shaper," *Opt. Lett.* **27**, 1345 (2002).
11. Z. Jiang, D. Leaird, and A. Weiner, "Optical arbitrary waveform generation and characterization using spectral line-by-line control," *J. Lightwave Technol.* **24**, 2487 (2006).

12. J. J. McFerran, W. C. Swann, B. R. Washburn, and N. R. Newbury, "Suppression of pump-induced frequency noise in fiber-laser frequency combs leading to sub-radian f_{ceo} phase excursions," *Appl. Phys. B* **86**, 219 (2007).
13. S. Zeller, T. Sudmeyer, K. Weingarten, and U. Keller, "Passively modelocked 77 GHz Er:Yb:glass laser," *Electron. Lett.* **43**, 32 (2007).
14. A. Schlatter, B. Rudin, S. C. Zeller, R. Paschotta, G. J. Spuhler, L. Krainer, N. Haverkamp, H. R. Telle, and U. Keller, "Nearly quantum-noise-limited timing jitter from miniature Er:Yb:glass lasers," *Opt. Lett.* **30**, 1536 (2005).
15. J. Schlager, B. Callicoatt, R. Mirin, N. Sanford, D. Jones, and J. Ye, "Passively mode-locked glass waveguide with 14-fs timing jitter," *Opt. Lett.* **28**, 2411 (2003).
16. F. Kärtner, J. der Au, and U. Keller, "Mode-locking with slow and fast saturable absorbers-what's the difference?" *IEEE J. Sel. Top. Quantum Electron.* **4**, 159 (1998).
17. C. Hönninger, R. Paschotta, F. Morier-Genoud, M. Moser, and U. Keller, "Q-switching stability limits of continuous-wave passive mode locking," *J. Opt. Soc. Am. B, Opt. Phys.* **16**, 46 (1999).
18. T. Schibli, E. Thoen, F. Kärtner, and E. Ippen, "Suppression of Q-switched mode locking and break-up into multiple pulses by inverse saturable absorption," *Appl. Phys. B* **70**, S41 (2000).
19. "MenloSystems, GmbH," URL www.menlosystems.com/fc1500.html.
20. B. Collings, K. Bergman, S. Cundiff, S. Tsuda, J. Kutz, J. Cunningham, W. Jan, M. Koch, and W. Knox, "Short cavity erbium/ytterbium fiber lasers mode-locked with a saturable Bragg reflector," *IEEE J. Sel. Top. Quantum Electron.* **3**, 1065 (1997).
21. S. Yamashita, Y. Inoue, K. Hsu, T. Kotake, H. Yaguchi, D. Tanaka, M. Jablonski, and S. Set, "5-GHz pulsed fiber Fabry-Perot laser mode-locked using carbon nanotubes," *IEEE Photonics Technol. Lett.* **17**, 750 (2005).
22. T. Schibli, K. Minoshima, H. Kataura, E. Itoga, N. Minami, S. Kazaoui, K. Miyashita, M. Tokumoto, and Y. Sakakibara, "Ultrashort pulse-generation by saturable absorber mirrors based on polymer-embedded carbon nanotubes," *Opt. Express* **13**, 8025 (2005).
23. "BATOP, GmbH," URL www.batop.de/products/saturable_absorber/SAM/SAMs_1550.html.
24. J. Townsend, W. Barnes, K. Jedrzejewski, and S. Grubb, "Yb³⁺ sensitised Er³⁺ doped silica optical fibre with ultrahigh transfer efficiency and gain," *Electron. Lett.* **27**, 1958 (1991).
25. B.-C. Hwang, S. Jiang, T. Luo, J. Watson, G. Sorbello, and N. Peyghambarian, "Cooperative upconversion and energy transfer of new high Er³⁺ - and Yb³⁺-Er³⁺-doped phosphate glasses," *J. Opt. Soc. Am. B, Opt. Phys.* **17**, 833 (2000).
26. Y. Hu, S. Jiang, T. Luo, K. Seneschal, M. Morrell, F. Smektala, S. Honkanen, J. Lucas, and N. Peyghambarian, "Performance of high-concentration Er³⁺-Yb³⁺-codoped phosphate fiber amplifiers," *IEEE Photon. Technol. Lett.* **13**, 657 (2001).
27. C. Jiang, W. Hu, and Q. Zeng, "Improved gain performance of high concentration Er³⁺/-Yb³⁺-codoped phosphate fiber amplifier," *IEEE J. Quantum Electron.* **41**, 704 (2005).
28. S. Grubb, W. Humer, R. Cannon, S. Vendetta, K. Sweeney, P. Leilabady, M. Keur, J. Kwasegroch, T. Munks, and D. Anthon, "24.6 dBm output power Er/Yb codoped optical amplifier pumped by diode-pumped Nd:YLF laser," *Electron. Lett.* **28**, 1275 (1992).
29. G. Vienne, J. Caplen, L. Dong, J. Minelly, J. Nilsson, and D. Payne, "Fabrication and characterization of Yb³⁺:Er³⁺ phosphosilicate fibers for lasers," *J. Lightwave Technol.* **16**, 1990 (1998).
30. M. Moenster, U. Griebner, W. Richter, and G. Steinmeyer, "Resonant saturable absorber mirrors for dispersion control in ultrafast lasers," *IEEE J. Quantum Electron.* **43**, 174 (2007).
31. D. Hanna, R. Percival, I. Perry, R. Smart, and A. Tropper, "Efficient operation of an Yb-sensitised Er fibre laser pumped in 0.8 μm region," *Electron. Lett.* **24**, 1068 (1988).
32. J. Sahu, Y. Jeong, D. Richardson, and J. Nilsson, "A 103 W erbium-ytterbium co-doped large-core fiber laser," *Opt. Commun.* **227**, 159 (2003).
33. G. Spühler, L. Krainer, E. Innerhofer, R. P. K. Weingarten, and U. Keller, "Soliton mode-locked Er:Yb:glass laser," *Opt. Lett.* **30**, 263 (2005).
34. B. R. Washburn, W. C. Swann, and N. R. Newbury, "Response dynamics of the frequency comb output from a femtosecond fiber laser," *Opt. Express* **13**, 10622 (2005).
35. N. Haverkamp, H. Hundertmark, C. Fallnich, and H. R. Telle, "Frequency stabilization of mode-locked erbium fiber lasers using pump power control," *Appl. Phys. B* **78**, 321 (2004).
36. H. Telle, "Stabilization and modulation schemes of laser diodes for applied spectroscopy," *Spectrochimica Acta Review* **15**, 301 (1993).

1. Introduction

Stabilized fiber-based mode-locked lasers (MLLs) have become a versatile tool in frequency metrology [1–5]. Moreover, there are a wide variety of additional applications including Fourier transform spectrometry [6–8], laser ranging [9] and arbitrary waveform generation [10, 11]. For

experiments in the 1.53-1.56 μm wavelength region, stabilized mode-locked fiber lasers (i.e., fiber laser frequency combs) typically have repetition rates of ~ 100 MHz. Many of these applications would benefit from having repetition rates nearer to 1 GHz. For example, the higher repetition frequency would provide a larger mode spacing of the resulting frequency comb, which is more suited to the resolution of many wavelength meters. In arbitrary waveform generation, the larger mode spacing would be much more compatible with current spectral dispersers. It is also envisaged that fiber lasers of higher repetition rate, due to their small size, could be used in a compact optical atomic clock as the read out mechanism.

In this paper we examine several aspects of high repetition rate, f_r , fiber lasers in the 1.54 μm wavelength region. First, can a fiber laser be fundamentally cw mode-locked with a repetition frequency beyond, say, 1 GHz using semiconductor saturable absorber mirror (SAM) technology? And if so, can such a system be phase-stabilized to the same degree as the more conventional lower repetition rate fiber lasers? Stabilization of passively mode-locked lasers requires stabilizing two degrees of freedom of the laser through two separate control parameters. One parameter is the cavity length; the other, and the one explored here, is modulation of the pump power to the laser. In particular, we are interested in whether the same technique of phase-lead compensated feedback to the pump power, successfully used for lower repetition rate fiber lasers [12], can be applied in stabilizing a high repetition rate laser.

Passively mode-locked lasers relying on Yb-Er phosphate glass as a gain medium have progressed rapidly in the past years, culminating in repetition rates as high as 77 GHz [13], and the timing jitter of related systems has been reduced to 190 fs [14]. A Yb-Er phosphate glass *waveguide* laser has been demonstrated with passive mode-locking at 750 MHz and a phase-locked timing jitter as low as 14 fs [15]. In addition, the theoretical models for such lasers, which use saturable absorbers, are also well understood [16–18].

A high f_r fiber laser, in contrast to a glass or crystal based laser, would be advantageous because it can be made from optical fiber components that are readily available, and it can be adapted to other systems via such components, producing a robust, flexible and relatively inexpensive apparatus. Previous efforts to produce high fundamental f_r fiber mode-locked lasers include a 250 MHz Er-doped fiber laser that uses non-linear polarization rotation to generate the mode-locking [19], a 175 MHz Er-doped soft-glass fiber laser that employs a saturable absorber mirror [2], and a co-doped Yb-Er fiber laser, again using a SAM, with a fundamental repetition frequency of 295 MHz [20]. More recently a Yb-Er fiber MLL with a saturable absorber formed from single-walled carbon nanotubes was developed where f_r reached 5 GHz [21]. While this approach seems very promising, the robustness of the carbon nanotubes needs to be improved before mode-locked lasers based on the technology become reliable over the long term [22].

Here, we have developed a fiber mode-locked laser with a fundamental repetition frequency as high as 2.08 GHz. The laser exhibits uniform intensity pulses exiting the cavity (i.e. cw mode-locking), and operates in the anomalous dispersion regime. Although the optical bandwidth is limited at present to about 2.6 nm, the laser is a preliminary demonstration of an energy efficient, compact and cost effective frequency comb. At $f_r=2.08$ GHz this represents the highest repetition rate of which the authors are aware for a fundamentally mode-locked fiber laser based on semiconductor saturable absorber technology. While there are many examples of high f_r harmonically mode-locked fiber lasers in the literature, the concept of a high f_r fundamentally MLL is attractive, primarily because there is greater leverage on the pulse-to-pulse timing jitter through cavity length control.

The outline of the remainder of the paper is as follows. Section 2 describes the design of two Yb-Er fiber laser cavities, one with an open air section and another without. Section 3 gives results pertaining to the lasers' model-locking behaviour. Sections 4 and 5 describe the stabilization of the repetition rate, and stabilization of a single comb tooth to a cavity-stabilized

cw laser, respectively. Finally, in Sect. 6 we briefly compare our results to the predictions of existing theoretical models.

2. Description of the mode-locked lasers

Two designs have been used to produce a mode-locked laser based upon Yb-Er fiber and a saturable absorber mirror. These are outlined in Fig. 1. The design of Fig. 1(a) was used for cavities with a variety of repetition rates ranging between 200 MHz and 1.05 GHz. In all cases, standard 1300-1550 nm single mode fiber (SMF) was fusion spliced to the end of a short length of less than 10 cm of Yb-Er fiber. Only a selection of these cavities is considered here (see below). A flat polished (PC) connector is placed on the Yb-Er fiber, an angle polished (APC) connector is placed on the SMF and a lens of 11 mm focal length and 0.25 NA was chosen to collimate the light exiting the SMF (for longer cavities the SMF was pre-mounted with a collimating optic). The collimated light is focused by a second lens (focal length = 4.5 mm, NA=0.5) onto the semiconductor SAM, where the spot size is $\sim 2.0 \mu\text{m}$ in radius. A standing wave cavity is formed between the SAM at one end and a partially reflective mirror at the input of the Yb-Er fiber, which acts as the output coupler. This output coupler, with a reflectivity of 98 % at 1550 nm, is optically gated to the fiber facet with the aid of index matching fluid.

The gain fiber is driven by an optically pumped semiconductor laser having a wavelength 975 nm and optical power 500 mW. After passing through coupling optics and an optical isolator the maximum power reaching the fiber laser cavity is about 380 mW (and the fraction of this light coupled into the Yb-Er fiber is about 70 %).

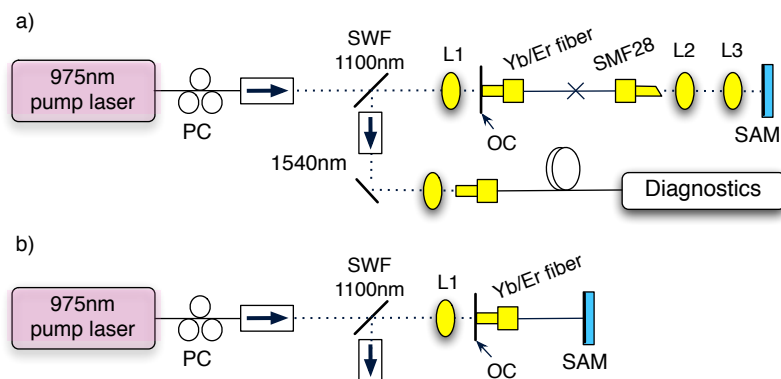


Fig. 1. Layout of two Yb-Er fiber lasers used in this work. They both form cw mode-locked lasers. SAM, (semiconductor) saturable absorber mirror; SWF, short wavelength pass filter; PC, polarization controller; OC, output coupler; L1 and L2, lenses with focal length = 11 mm; L3, lens with focal length = 4.5mm. Solid lines represent fiber, and dotted lines, air paths.

The alternative set up shown in Fig. 1(b) was used to get an appreciation of the repetition rates that are achievable using a Yb-Er fiber plus SAM system. Here the SAM is simply butted up against the cleaved end of about 5 cm of Yb-Er fiber. Although not nearly as robust as that of Fig. 1(a), the design could be modified to make a rugged laser using presently available fiber-to-SAM mounting technology [23].

The gain medium of the laser is a phosphosilicate fiber of core-pumped geometry, co-doped with ytterbium and erbium ions. The Yb^{3+} absorbs 975 nm pump light, then transfers the energy to the Er^{3+} via lattice vibrations in the phosphor doped host with a transfer efficiency

as high as 95 % [24, 25]. Optical amplifiers using Yb-Er fiber have demonstrated gains of 5 dB/cm [26], and a gain of 8.6 dB/cm is predicted to be achievable with optimum co-doping concentrations [27]. Furthermore, optical conversion efficiencies of 38 % have been generated in similar systems (pumped at $\lambda \sim 1060$ nm) [28]. Unlike Yb-Er waveguide or glass lasers, the Yb-Er fiber host is predominantly silica and not phosphate glass. The advantage is that the commercially available fiber (e.g. DF1500Y from Fibercore) can be readily fusion spliced to standard single mode fiber, provided the phosphate content is not too high. However, the dopant concentrations are proportional to the phosphate content [29]. This then limits the concentration of Yb and Er ions; here, the ion concentrations are $[\text{Er}^{3+}] \sim 4 \times 10^{18} \text{ cm}^{-3}$ and $[\text{Yb}^{3+}] \sim 1.8 \times 10^{20} \text{ cm}^{-3}$, giving a Yb:Er ion concentration ratio of 45. The small signal absorption is ~ 1000 dB/m at 980 nm and 20 dB/m absorption at 1535 nm. Dispersion measurements of the Yb-Er fiber give $\beta_2 = +14.0 \pm 0.2 \text{ ps}^2/\text{km}$ at 1540 nm.

The SAM acts as the nonlinear absorption element in the cavity that initiates and maintains the pulsed behaviour. We have carried out experiments with two semiconductor SAMs: one, which we denote as SAM_{0.11}, has a relatively strong modulation depth (i.e., maximum change of reflectivity) of $\Delta R = 11$ %, and the other, denoted SAM_{0.012}, has a weak modulation depth, $\Delta R = 1.2$ %, but a correspondingly low nonsaturable loss. Their characteristics are listed in Tab. 1. (These values are manufacturer specifications. Our own measurements for SAM_{0.11} showed relatively close agreement, while SAM_{0.012} was not tested.) SAM_{0.11} has a resonant design [30] and SAM_{0.012}, an antiresonant design.

Table 1. Semiconductor saturable absorber characteristics.

Designation	Saturation fluence, $\mu\text{J}/\text{cm}^2$	Modulation depth	Nonsaturable loss	τ_A^a , ps	GDD ^b at 1540 nm, fs ²
SAM _{0.11}	20	0.11	0.09	2	-2.0×10^3
SAM _{0.012}	70	0.012	0.008	~ 10	20

^a Relaxation time constant

^b Group delay dispersion

SAM_{0.11}, with the relatively high ΔR , is conducive for pulsed fiber lasers where the laser mode-locks in the fast saturable absorber regime. In this regime the pulse width is expected to narrow for stronger modulation depths (see Eq. 1 below). Laser cavities using this SAM generated cw mode-locking with repetition rates as high as 2.08 GHz. SAM_{0.012} was chosen to test the significance of reducing linear loss in the cavity with the prospect of producing a wider bandwidth laser output, as discussed later.

Table 2. Fiber length combinations and net group delay dispersion for different cavities.

f_r^a	Yb-Er fiber length (cm)	SMF length (cm)	OAS ^b length (cm)	Cavity GDD ^c (fs ²)
535 MHz	8.5	8.5	2.5	-2900
860 MHz	8.0	2.5	2.5	-730
1.01 GHz	5.5	2.5	2.5	-1430
2.08 GHz	4.8	0	0	-660

^a Fundamental repetition frequency

^b Open air section

^c Group delay dispersion; calculated for SAM_{0.11}

All of the lasers considered in this paper have their component lengths listed in Tab. 2 and apart from the 2 GHz MLL they all use the design of Fig. 1(a). It is worth noting that cw mode-locking was achieved with solely Yb-Er fiber in the Fig. 1(a) configuration, but there were difficulties avoiding what we suspect were higher order spatial modes resonating in the open air section. For the four cavities listed in Tab. 2 the net cavity group delay dispersion (GDD) is

computed (a dispersion value of $\beta_2 = -19.5\text{ps}^2/\text{km}$ is assumed for the SMF, and only $\text{SAM}_{0,11}$ is considered). They all have net anomalous dispersion, providing one necessary condition for quasi soliton mode-locking.

3. CW mode-locking at 1 and 2 GHz

A series of measurements pertaining to the $f_r=1.01$ GHz Yb-Er fiber laser are displayed in Fig. 2. The microwave spectrum of Fig. 2(a) shows the repetition rate signal and its harmonics out to a frequency of ~ 13 GHz. For $f_r=1.01$ GHz the corresponding round-trip time of 1 ns agrees closely with that expected for a SMF plus Yb-Er fiber length of 8 cm and OAS length ≈ 2.5 cm. The nearly uniform intensity of the harmonics demonstrates that the laser is mode-locking with a single pulse propagating through the cavity (the irregular noise floor is due to the spectrum analyzer). Fig. 2(b) displays f_r with a span of 10 MHz, showing the absence of sidebands associated with amplitude modulation of the pulse train, i.e., Q-switching (the associated sidebands occur at ~ 1 MHz for this cavity when the pump power is insufficient). From Fig. 2(c) we see that a train of pulses emitted from the laser exhibits constant amplitude, again indicating cw mode-locked behaviour. The small variation in pulse height can be attributed to the insufficient resolution of the oscilloscope. Closer examination of the individual pulses, both with a 50 GHz oscilloscope and an autocorrelator, shows no sign of pulse break-up. The final plot in Fig. 2(d) displays the optical spectrum of the laser light, which closely adheres to a Gaussian line-shape with a FWHM of 2.6 nm.

These results were produced with 2 % output coupling, and the corresponding average optical power exiting the cavity was about 1.3 mW with linearly polarized light. Fine adjustment of the lens directing light onto the SAM could induce a degree of elliptical polarization (as made manifest by weak interharmonic modes). The APC connector provides a weak selection effect for linear polarization, but if this proves inadequate, a low loss linear polarizer can also be placed in the cavity to enforce linear light polarization.

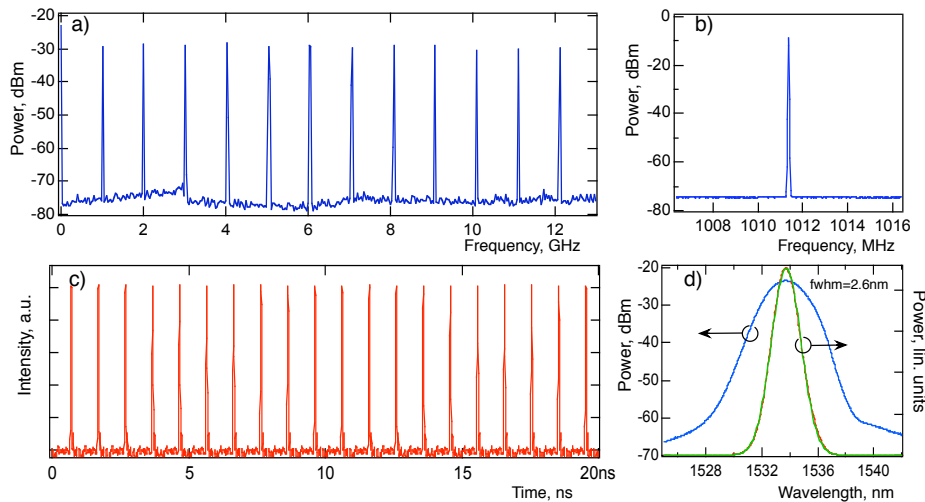


Fig. 2. Measurements of the 1.01 GHz Yb-Er fiber laser. (a) Microwave spectrum with multiple harmonics of f_r . (b) Field spectrum of f_r with a 10 MHz span and res. bandwidth = 10 kHz. (c) Pulse train (d) Optical spectrum: the green trace is a Gaussian fit to the linear profile of the measured red trace beneath, while blue trace shows the spectrum on a logarithmic scale.

At this high repetition rate the extent of the Q-switched mode-locking (QML) regime is very small in terms of pump power range, unlike the situation for longer cavities. As the pump power is reduced to about 200 mW the onset of Q-switching is closely followed by complete mode-locking failure. Thus, there is a rapid transition between pure amplified spontaneous emission and cw mode-locking.

There are reports of Yb³⁺ ion lasing in core pumped Yb-Er fiber lasers [31] and in cladding pumped Yb-Er fiber lasers [32]. However, we find that under mode-locked conditions the laser is completely free from lasing of the sensitizing ion (suggesting that the reflectivity at 1030 nm of the end reflectors is suitably low).

For some applications an output of larger bandwidth (shorter pulse) is advantageous. One method for producing a pulse of broader bandwidth is to broaden the gain bandwidth. The gain bandwidth of the laser is governed predominantly by the emission cross section of the Yb-Er fiber and the level of inversion; a lower inversion (lower gain) will result in a broader gain bandwidth [33]. Computations, along with measured emission and absorption profiles for the Yb-Er fiber, suggest that a 60 % inversion level is required to produce a 35 nm gain bandwidth. To explore the effects of reduced cavity loss, we investigated mode-locking with the $\Delta R = 1.2\%$ SAM. In the anomalous dispersion regime the output spectrum closely followed the expected sech^2 line shape, indicative of soliton mode-locking. However, the spectral width was limited to 0.32 nm, considerably less than the 2.6 nm achieved with SAM_{0.11} (presumably due in part to the decreased ΔR).

In the work of Collings *et al.* [20], there was strong dependence of spectral width upon fiber length. Using SAM_{0.11} with 9 % non saturable loss and a 2 % output coupler we found only a small dependence of laser light spectral width upon Yb-Er fiber length. For example, the -3 dB spectral width of the MLL light increased from 1.3 nm to 2.6 nm for a change in Yb-Er fiber length of 9.5 cm to 5.5 cm, respectively. We suspect that the cavity losses in our system are too high relative to those of Ref. [20]. Another factor could be the difference in the ratio of compounds making up the host glass, since different core compositions can affect the absorption and emission cross sections [24].

To examine the effects of dopant concentration ratios, a laser cavity composed of fiber with [Yr³⁺]:[Er³⁺] = 20:1, rather than 45:1, was tested with lengths of Yb-Er fiber and SMF similar to those used in the $f_r=860$ MHz cavity. There was little difference in both the behaviour of the laser observed and the pulse spectral width, suggesting that the change in Yb:Er ratio (in this case due to an increase in Er³⁺) has little influence on the emission spectrum.

A selection of the microwave spectra recorded for two slightly different length Yb-Er fiber lasers with f_r near 2 GHz is shown in plots (a) to (d) of Fig. 3. Apart from the slight difference in f_r in figures (a) and (b), one also notices sidebands on the repetition frequency signal and its harmonics in Fig. 3(b). These are not Q-switching sidebands, but instead arise because the light is not completely linearly polarized. Between cavity setups the degree of linear polarization can change slightly. Figure 3(c) shows f_r with a span of 50 MHz (resolution bandwidth (RBW) of 100 kHz). At insufficient pump power the sidebands associated with Q-switching appear up to ~ 5 MHz away from the carrier (unlike the situation here). Figure 3(d) examines the field spectrum of f_r at frequencies closer to the carrier. At a RBW of 300 Hz there still remains a narrow carrier signal, which bodes well for high frequency resolution applications. The optical spectrum is displayed in Fig. 3(e), again with both logarithmic and linear scales. We note that the spectral width is little changed from the $f_r=1$ GHz system. The average optical power emitted by this cavity with 2 % output coupling is approximately 2 mW with an estimated 280 mW of pump light entering the gain medium. Attempts with an $f_r=2.5$ GHz cavity failed to produce cw mode-locking (with SAM_{0.11}).

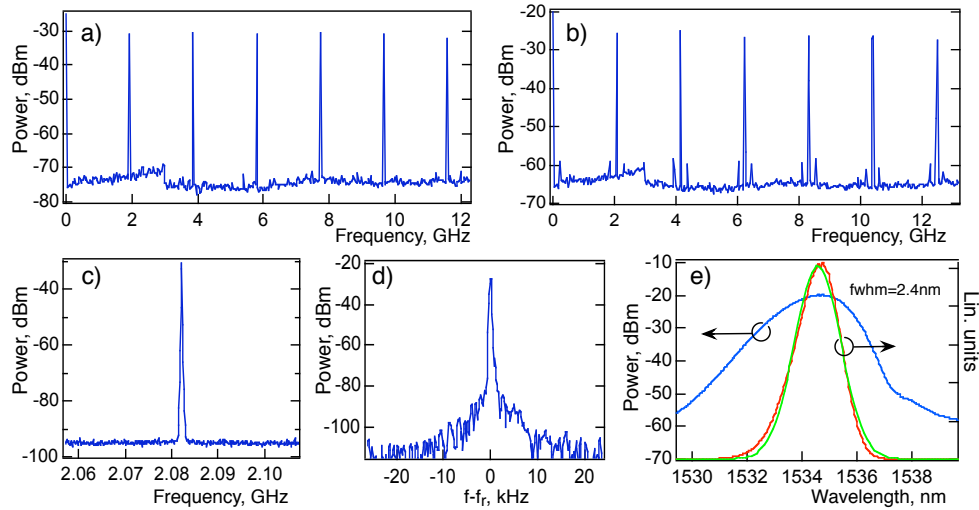


Fig. 3. Measurements of the Yb-Er fiber laser with f_r near 2 GHz (using the $\Delta R = 0.11$ SAM). (a) Microwave spectrum with multiple harmonics of f_r . (b) Similar to (a), but showing sidebands that are a manifestation of slightly elliptically polarized light. (c) Field spectrum of f_r with a 50 MHz span and RBW = 100 kHz. (d) f_r at RBW = 300 Hz (e) Optical spectrum: the green trace is a Gaussian fit to the linear profile of the measured red trace beneath.

4. Stabilization of the repetition rate

The response function of the MLL's output intensity with respect to the current modulation of the pump laser was measured, as shown in Fig. 4(a). This response function maps directly to the modulation of the repetition frequency through a variety of effects [12]. We find that the -3 dB roll-off frequency, $f_{-3\text{dB}}$, occurs at ~ 1.8 kHz, which is indicative of a laser with very stable mode-locking [34]. There are no relaxation oscillations, instead the modulation response falls with the same characteristic as a single pole low pass filter, so the phase can be readily compensated in a negative feedback control system, as similarly carried out for nonlinear-polarisation-rotation (NPR) fiber lasers [12]. To demonstrate this we stabilize the repetition rate via feedback to the pump laser. More typically, f_r is stabilized through control of the cavity length, but pump power has been used to stabilize the repetition rate of a ring fiber laser previously [35].

The f_r noise was suppressed by heterodyning a filtered $2 \times f_r$ signal with a low-noise microwave signal and using the low-pass filtered mixer output to modulate the pump laser current via an N-channel JFET [36] (with some derivative feedback to increase the phase margin beyond $f_{-3\text{dB}}$). In Fig. 4(b) the one-sided phase spectral density, S_ϕ , of the 2nd harmonic of a $f_r = 535$ MHz Yb-Er mode-locked laser is shown under free running (red trace) and closed loop operation (blue trace). The corresponding timing jitter spectral density is shown on the right axis. The closed-loop noise was measured with a separate mixer, outside the servo loop (and internal to the vector signal analyzer recording the phase noise). The servo peak at 40 kHz shows how the servo bandwidth can be pushed well beyond the roll-off frequency of the MLL. The integrated timing jitter of the closed-loop signal is 100 fs for the frequency range shown, or 30 fs if one disregards the servo peak (which was enhanced to elucidate the servo bandwidth). This is a promising result considering that the measured closed loop noise is masked by the measurement noise floor. Here, the servo is engaging the pump laser to compensate for, in the majority, cavity length variations caused by environmental disturbances. Usually these

fluctuations are controlled via piezo actuation of an end reflector or by fiber stretching. However, the servo operation seen here demonstrates that the carrier-envelope offset frequency of the MLL, if extracted, could be adequately controlled. It further shows that the Yb-Er laser's mode-frequency response is not unlike that of NPR Er doped fiber lasers; often used as frequency comb devices. Note that passive reduction of this timing jitter would likely be achieved by applying a reflection coating directly to the fiber input, rather than pressing the output coupler against the input of the fiber.

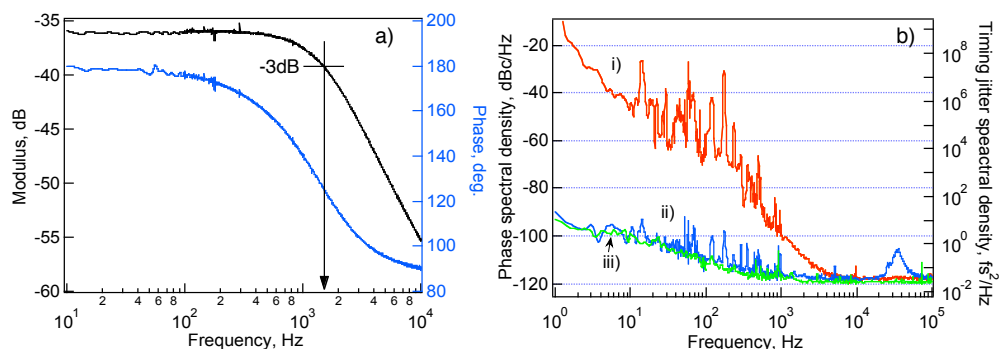


Fig. 4. (a) Response function of the MLL's output intensity with respect to the current modulation of the pump laser. (b) One-sided phase spectral densities of the $2 \times f_r = 1.07$ GHz signal of a cw mode-locked Yb-Er laser. Trace (i), open loop; (ii), closed out-of-loop; and (iii), measurement system noise floor. The right axis shows the corresponding timing jitter spectral density.

5. Stabilization of a single comb tooth

Another test demonstrating the versatility of the Yb-Er laser was to phase-lock one of the teeth of the frequency comb to a cavity-stabilized cw laser at $1.535 \mu\text{m}$. The optical signals of the cw light and a $f_r = 850$ MHz MLL were combined on a photodetector generating an rf beat signal, which was then filtered, amplified and divided before heterodyning with a local oscillator in a digital phase-locked loop. The loop-filtered correction signal then modulated the pump laser

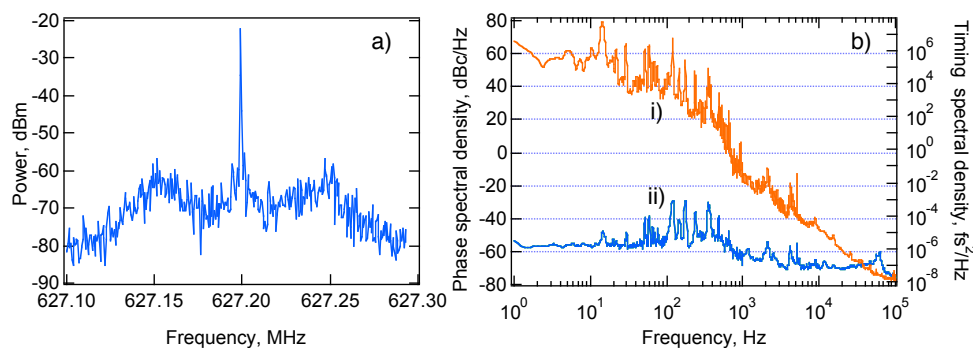


Fig. 5. (a) Field spectrum of a phase-stabilized optical beat signal, RBW= 300 Hz (b) One-sided phase spectral density of the 627 MHz beat signal when (i) unstabilized and (ii) phase-locked. The right axis shows the corresponding timing jitter spectral density.

current as before. The field spectrum of the locked beat signal is displayed in Fig. 5(a), while Fig. 5(b) shows the open loop (upper trace) and closed in-loop phase spectral densities. The phase-lead compensation (derivative feedback) and loop filtering has had an even more pronounced effect here with the servo peak now at 60 kHz. The timing jitter spectral density, normalized by the 194 THz carrier frequency, is shown on the right axis of Fig. 5(b). The integrated timing jitter of the phase-locked beat signal, for the frequency range shown, is 0.22 fs and the corresponding integrated phase noise is 0.06 rad². A rigorous out-of-loop measurement of the pulse timing requires two fully phase-locked MLLs, which are not available at present, but the above results indicate sub-Hz linewidths should be possible from a fully phase-locked system.

A measurement of the f_r noise recorded while the optical beat was phase-locked showed little change from its open-loop phase noise. The most likely explanation for this is that the fixed point of the frequency comb with respect to pump laser intensity fluctuations is separated significantly from the comb mode producing the beat signal. The fact that the beat signal is very sensitive to pump laser fluctuations (~ 12 MHz/mW) supports this. To verify this separation, we measured the fixed point for pump-power fluctuations by measuring df_{beat}/dP and df_r/dP , where P represents pump power. From these two quantities we can extract df_{ceo}/dP , from the ratio of df_{ceo}/dP to df_r/dP we find the fixed point mode number to be $\sim 380 \times 10^3$ (for the $f_r=860$ MHz laser), corresponding to a wavelength of ~ 920 nm.

6. Comparison with models

With regard to mode-locked lasers there are four possible regimes of operation: either fast or slow saturable absorption with either solitonic or nonsolitonic mode-locking. With respect to the nature of the saturable absorption, if the saturable absorber time, τ_A , is not much greater than the pulse width, τ_P , then the laser operates in the fast saturable absorber regime [18]. In our case, the maximum spectral widths of the laser with SAM_{0.11} and SAM_{0.012} are ~ 2.6 nm and 0.6 nm, respectively. As an approximation, if we consider the transform limited situation, the corresponding FWHM pulse widths are 1.3 ps and ~ 6 ps, which lie just below the relaxation times of the respective saturable absorbers. It is then inferred that the laser operates in the fast-saturable absorber regime irrespective of the SAM employed. As further validation of this, we consider the expression relating SAM modulation depth to pulse width for the case of a fast saturable absorber [16, 18]. Here we have,

$$\tau_{P, FSA} = 1.76 \left(\frac{2g}{\pi^2 \Delta v_g^2 \Delta R} \right)^{1/2} \quad (1)$$

where $\tau_{P, FSA}$ is the FWHM pulse width, g is the power gain per round trip at the central wavelength, and Δv_g is the FWHM of the gain bandwidth (the HWHM gain bandwidth denoted as Ω_g in Ref. [18] is equal to $\pi \Delta v_g$). Gain filtering is the dominant filter mechanism here. The values of these and other relevant parameters are listed in Tab. 3. Our estimate for the gain bandwidth, based on our measurement of the gain fiber's emission spectrum, is ~ 18 nm (although strictly it is expected that there will be a difference for the two SAMs). Then Eq. 1 yields $\tau_P \sim 1.3$ ps and 4 ps for the SAM_{0.11} and SAM_{0.012} cavities, respectively; similar to the transform-limited pulse widths.

The importance of solitonic effects is quantified by the ratio of the saturable absorption coefficient, γ , and the self-phase modulation coefficient, δ [16]. The former is given by $\gamma = \tau_A \Delta R / (F_{sat, A} A_A)$, where τ_A and $F_{sat, A}$ are the relaxation time and saturation fluence of the absorber, respectively, and A_A is the mode area of the light impacting on the SAM. The self-phase modulation coefficient is given by $\delta = 2\pi n_2 L_K / (\lambda_0 A_L)$, where n_2 is the nonlinear refractive index, L_K is the length of the Kerr medium per round trip, A_L is the effective mode

area of the Kerr medium, and λ_0 is the center wavelength. For the $f_r=1$ GHz Yb-Er MLL with SAM_{0,11}, $\gamma/\delta \sim 80$ (using the round trip fiber length for the Kerr medium). For the same laser, but with SAM_{0,012}, $\gamma/\delta \sim 40$. So in both situations the saturable absorber would seem to be the dominant mechanism for pulse stabilization, and the laser operates in the non-solitonic regime (NSR). It is worth noting, however, that when the length of the gain medium plus SMF is increased to 18 cm (with SAM_{0,012}), the ratio drops to $\gamma/\delta \sim 1.5$ and the spectral line shape becomes hyperbolic secant, consistent with the laser producing solitonic mode-locking.

Table 3. Parameter description and values for the Yb-Er mode-locked laser.

Symbol	Quantity	Value
[Er ³⁺]	Erbium ion concentration	$4 \times 10^{18} \text{ cm}^{-3}$
[Yb ³⁺]	Ytterbium ion concentration	$1.8 \times 10^{20} \text{ cm}^{-3}$
A_L	Effective mode area of gain medium	$27 \mu\text{m}^2$
A_A	Effective mode area on saturable absorber	DoC ^a
D_2	Net group delay dispersion	DoC
$\Delta\nu_g$	Gain bandwidth (FWHM)	2.3 THz (18 nm)
ΔR	Modulation depth of saturable absorber	0.11
$F_{sat,L}$	Gain medium fluence	7.2 J/cm^2
g	Gain per round trip	1.5
L_K	Length of the Kerr medium per round trip	DoC
λ_0	Central wavelength	1535 nm
n_2	Nonlinear refractive index	$4.5 \times 10^{-20} \text{ m}^2/\text{W}$ ^b
σ_L	Emission cross section at 1535 nm	$9 \times 10^{-21} \text{ cm}^2$
T_{OC}	Transmission of output coupler	2 %

^a depends on the cavity under consideration

^b assumed to be similar to that of silica fiber

A common behaviour of mode-locked lasers, especially those incorporating semiconductor saturable absorbers, is Q-switched mode-locking, where there is strong amplitude modulation of the emitted pulse train. Typically a threshold pulse energy must be reached to suppress Q-switching and keep the laser cw mode-locked. Indeed, one of the main motivations for this work was to establish whether cw mode-locking was robust in a GHz-repetition rate Yb:Er fiber laser system. The initial work by Hönninger *et al.* [17] considered the effects of the saturable absorber and saturation of the gain medium. Using their expression, we find a threshold output power of 12 mW, or ~ 20 times greater than the measured value of 0.61 mW for our 860 MHz repetition rate laser. From this result, one may interpret that the pulse behaviour is not governed simply by saturation effects of the gain medium and absorber. Again following Ref. [17], solitonic effects will reduce the saturation power significantly. However, it is more likely that additional damping mechanisms in the SAM are the dominant stabilization mechanism, as discussed by Schibli *et al.* [18]. They include the influence of two-photon and free-carrier absorption that cause a roll-off in the SAM response with increasing power. The necessary parameters for our SAM are not available, but our threshold pulse energy for cw mode-locking of ~ 40 pJ is not unreasonable with the model described in Ref. [18]. This is a topic for further investigation.

7. Conclusions

We have developed a mode-locked laser based on ytterbium-erbium co-doped fiber with a pulse repetition rate as high as 2.08 GHz at a central wavelength of $1.535 \mu\text{m}$. The laser, with an 11 % modulation depth SAM, contains a single pulse per round trip and is free of Q-switching instabilities and higher spatial mode resonances. This is the first report of a semiconductor saturable

absorber based fiber laser producing fundamentally mode-locked repetition rates greater than 1 GHz. The maximum spectral bandwidth of the light emitted from the cavity is 2.6 nm, which we determine to be limited by the SAM, because the laser appears to operate in the fast saturable absorber regime. For the $f_r=2$ GHz mode-locked laser, where the Yb-Er fiber is butted directly to the SAM, the set up is not robust, but improvements should be straightforward since more reliable schemes are already available commercially [23].

In an alternative arrangement that produces a reliable and self starting cw mode-locking, the gain fiber was spliced to single-mode fiber; the light from the fiber was collimated and then focused onto the SAM. Here we still achieve repetition rates greater than 1 GHz. Despite there not being much fiber, it can still be connectorized or spliced and thus coupled together easily with other optical fiber components. Thus, like more conventional fiber mode-locked lasers, it is a robust, flexible and an easily adaptable optical system.

A comb tooth of a $f_r=850$ MHz Yb-Er MLL was locked to a low-noise, cavity-stabilized cw laser at $1.535 \mu\text{m}$ by use of electronic feedback to the pump laser current. Phase-lead compensation helped produce a servo bandwidth of more than 60 kHz, well beyond the 1.8 kHz response bandwidth of the laser, with an in-loop timing jitter of 0.22 fs between 1 Hz and 100 kHz. The laser therefore exhibits the potential for generating a very low-noise frequency comb. A fully self-referenced frequency comb will likely require a large output bandwidth. It is noted that most of the SAM based MLLs that achieve pulses much narrower than the relaxation time of the saturable absorber tend to have short crystal or glass gain media with Kerr-lens mode-locking occurring, or, in the case of fiber, employ a form of additive pulse mode-locking. However, several possibilities exist for increasing the bandwidth of the laser here, including a SAM with even larger modulation depth or gain-flattening filters to provide a broader gain bandwidth.

Acknowledgements

The authors thank Ellen Landis of Fibercore for information regarding the Yb-Er fiber, Dr Wolfgang Richter of BATOP, GmbH, for information about the saturable absorber mirrors, and Bookham for providing gain-flattening filter chips. We are highly indebted to T. Schibli for informative discussions, to S. Etzel and I. Coddington for technical assistance, and to S. Diddams, L. Hollberg, P. Williams and T. Dennis for the loan of equipment.

Declaration: Manufacturers of certain products are identified in this paper for technical clarity only. Inclusion in this paper implies neither endorsement by NIST nor that similar but different implementation of the product will perform equally well.